

Modeling, Analysis, and Prediction of Flutter at Transonic Speeds

K.-Y. Fung* and T. H. Shieh†
University of Arizona, Tucson, Arizona 85721

The solutions of the two-degree-of-freedom aeroelastic system of an airfoil about different elastic axes are shown to be algebraically homomorphic. A simple aerodynamic model allows the characterization of this system by the lift and moment slopes and two characteristic time constants from the indicial response to pitch, in addition to the usual structural parameters. Algebraic expressions for the flutter speed and frequency in terms of these parameters are thus derived. For flutter frequencies that are small compared with the characteristic time constants or for time constants that are close in magnitude, these expressions can be further simplified to uncoupled, explicit expressions. Many characteristics of flutter and their parametric dependency are readily discernible from these expressions, including the condition for flutter. It is shown that the flutter speed reaches the minimum (the so-called transonic dip) as the slope of pitching (about midchord) moment curve C_{m_α} becomes maximum. Hence, the Mach number of the transonic dip is predictable using quasisteady aerodynamics. Examples are also given to show the applicability of this simple criterion for the transonic dip of supercritical wings.

Nomenclature

a	= distance in semichords of elastic axis behind midchord
b	= semichord
C_{l_α}, A_1	= lift-curve slope
C_{m_α}, A_3	= slope of pitching moment curve for midchord axis
c	= chord length
g	= structural damping factor
h	= vertical displacement of elastic axis (positive downward)
i	= complex constant, $\sqrt{-1}$
K	= key parameter for flutter, $4A_3A_4/r_\alpha^2A_1$
K_h	= flexure spring constant
K_α	= torsion spring constant
k, k_c	= reduced frequency based on full chord, $\omega c/U_\infty$
k_b	= reduced frequency based on semichord
L	= lift per unit span (positive up)
L_1	= lift coefficient due to plunging
L_2	= lift coefficient due to pitching
M_y	= pitching moment per unit span about elastic axis (positive nose up)
M_∞	= freestream Mach number
M_1	= moment coefficient due to plunging
M_2	= moment coefficient due to pitching
m	= mass per unit span
R	= uncoupled frequency ratio, ω_h/ω_α
r_α	= radius of gyration in semichords about elastic axis
t	= dimensionless time measured by chord lengths traveled
U, U_∞	= flutter speed, freestream velocity
\bar{U}	= $(U/c\omega_\alpha)^2$
X_b	= distance in semichords of center of gravity from elastic axis
X_{cg}	= distance in semichords of center of gravity from midchord
Z	= flutter solution, $(\omega_\alpha/\omega)^2(1 + ig)$

α	= angular displacement, angle of attack
β	= arbitrary constant
λ_l^{-1}, A_2	= characteristic time of lift response to pitch
λ_m^{-1}, A_4	= characteristic time of moment response to pitch
μ	= mass ratio, $m/(\pi\rho_\infty b^2)$
ρ	= μ/μ'
ρ_∞	= freestream density
ω, ω_F	= circular flutter frequency
ω_h, ω_α	= uncoupled natural frequencies for plunging and pitching, respectively

Subscripts

i	= imaginary part of a complex quantity
r	= real part of a complex quantity
∞	= property of freestream

Superscript

' = quantities with respect to pitching about midchord

Introduction

IT has been known since World War II that wings and control surfaces of high-speed aircraft are most unstable, aeroelastically, at transonic speeds and that the lowest flutter dynamic pressure of many wings of advanced design occurs at a Mach number near unity. The sudden rise in the flutter dynamic pressure was noted in early experiments on rocket-propelled or free-falling objects and attributed to the shift in the dynamic center of pressure associated with two-dimensional supersonic flow, but the Mach number at which the rise begins was found to be sensitive to wing thickness among other factors.¹ Landahl² in the introduction of his monograph emphasized the importance of large phase lags between motion and air pressures at transonic speeds. The comprehensive work and careful experiments of Tijdeman³ led many researchers to focus their attention on shock motion and ascribe it to the sudden drop in flutter dynamic pressure as the flow becomes supercritical. Isogai^{4,5} asserted that the transonic dip is caused by the large time lag between the aerodynamic pressure and the airfoil motion due to compressibility effects, especially the phase delay of the shock motion. He also exemplified the dominance of single-degree-of-freedom flutter at the dip. Ashley⁶ assessed the role of shocks by adding, heuristically, a shock-force doublet to the forces given by classical theory. Zwaan⁷ attributed the mechanism of flutter to the

Received July 16, 1991; revision received May 29, 1992; accepted for publication June 5, 1992. Copyright © 1991 by K.-Y. Fung and T. H. Shieh. Published by the American Institute of Aeronautics and Astronautics, Inc., with permission.

*Associate Professor, Department of Aerospace & Mechanical Engineering, Member AIAA.

†Ph.D. Candidate; currently, NRC Research Fellow, NASA Johnson Space Center, Mail Code EG3, Houston, TX 77058.

large phase lag in the lifting force due to pitching and hypothesized that the dip should be determined primarily by this lag. In an attempt to account for the substantially lower flutter boundary found in the experiments of the supercritical TF-8A wing than that of the same wing except with conventional cross sections, Farmer and Hanson⁸ noted the marked increase in the lift-curve slope of the former over that of the latter wing and commented that the dynamic pressure at flutter tends to be proportional to the inverse of the lift-curve slope.

For flutter analysis of subsonic or supersonic flight, reliable methods based on linearized theories are readily available.^{9,10} The difficulty of an analysis involving a transonic flow lies in the well-known intrinsic transonic nonlinearity, which makes any linearized theory amplitude dependent and, hence, its validity restricted to special cases. Since the advent of the modern computer, the majority of research and developments in steady and unsteady transonic flows has focused on the numerical approach. It is a common expectation that this alternative to wind-tunnel testing would become more economically feasible as the computer becomes more powerful. Nevertheless, even with all of the expected advances in both hardware and software, the costs of a flutter analysis for a transonic flight using the numerical approach remain prohibitively high for routine applications. The lack of an engineering approach with effective characterization of the transonic nonlinearity has precluded configuration optimization for the transonic speed range in the preliminary design.

A typical flutter analysis involves a set of parameters characterizing the structural properties of the wing, or wing section, and the aerodynamic response as a function of the structural deformation modes. Because of the functional complexity in the aerodynamic response, an analysis of the simplest flexure-torsion flutter of an airfoil in an incompressible flow amounts to a task of finding the complex roots of an algebraic system, containing complex transcendental functions, through numerical means.¹¹ For a subsonic flow, the exact functional representation of the aerodynamic response, e.g., to pitching, is not known, and approximations valid for low reduced frequencies are also in terms of complex transcendental functions.¹² For a transonic flow, the aerodynamic response function itself is known to exist only as a numerical approximation to the governing equation,¹³ and an analysis amounts to pointwise solution evaluations in a restricted region of the parametric solution space.

Here, the aerodynamic model of Fung¹⁴ is used to represent the aerodynamic response to pitching and plunging of an airfoil in a transonic flow. It will be shown that the low frequency assumption implied in the model and the large characteristic time of the aerodynamic response render simple, explicit, algebraic expressions for the flutter speed and flutter frequency in terms of the structural parameters, the slopes of the lift and pitching moment curves, and two time constants characterizing the lift and moment responses to indicial pitch. Evaluations and comparisons with published results show that these expressions, despite their simplicity and explicitness,

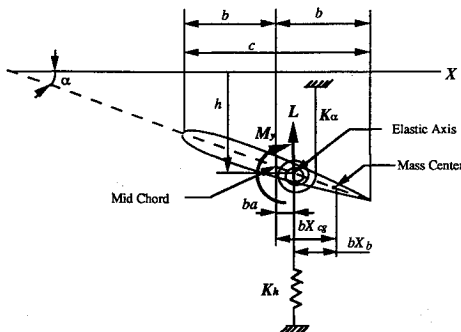


Fig. 1 Definition of parameters for two-degree-of-freedom flutter system.

preserve the essential parametric dependency of the aeroelastic system and deviate very little from the classical approach.

An important result of these expressions is that the transonic dip occurs when the slope of the pitching moment curve, C_{m_α} is stationary with respect to the Mach number. This criterion, being purely aerodynamic and derived for airfoils, seems to hold for wings as well.

Homomorphic Flutter System

The classical flutter analysis of a two-degrees-of-freedom airfoil system, Fig. 1, amounts to finding the complex roots Z of the determinant (e.g., see Ref. 15),

$$\begin{vmatrix} \mu(1 - R^2 Z) + L_1 & \mu(X_{cg} - a) + L_2 \\ \mu(X_{cg} - a) + M_1 & \mu r_\alpha^2(1 - Z) + M_2 \end{vmatrix} = 0 \quad (1)$$

where μ is the ratio of airfoil mass to apparent mass of air, R the ratio of uncoupled (plunging to pitching) circular frequencies, a the distance of the elastic axis about which the radius of gyration r_α is measured, X_{cg} the location of the center of gravity (all distances measured in percent half-chord from midchord), and L_1 , L_2 , M_1 , and M_2 are lift and moment coefficients (in complex form) corresponding to plunging and pitching modes, subscripts 1 and 2, respectively. The first five parameters are essentially structural, and the last four are purely aerodynamic. The solution Z is related to the flutter circular frequency ω and structural damping factor g (normally set to zero for a critical flutter analysis) by $Z = (\omega_\alpha/\omega)^2(1 + ig)$, where i is the complex constant. Standard procedures for solving Eq. (1) are well established (e.g., the U - g method¹⁵) and need no further explanation here.

The aerodynamic coefficients L_1 , L_2 , M_1 , and M_2 obtained for the elastic axis position a can be related to those obtained for the midchord by

$$\begin{bmatrix} L_1 \\ L_2 \\ M_1 \\ M_2 \end{bmatrix} = \begin{bmatrix} 1 & 0 & 0 & 0 \\ -a & 1 & 0 & 0 \\ -a & 0 & 1 & 0 \\ a^2 & -a & -a & 1 \end{bmatrix} \begin{bmatrix} L'_1 \\ L'_2 \\ M'_1 \\ M'_2 \end{bmatrix} \quad (2)$$

Herein, the prime denotes quantities with respect to midchord, $a = 0$. Equation (1) can be rewritten in the form

$$[D, -C, -B, A] \begin{bmatrix} L_1 \\ L_2 \\ M_1 \\ M_2 \end{bmatrix} = BC - AD \quad (3)$$

where

$$\begin{aligned} A &= \mu(1 - R^2 Z) \\ B &= \mu(X_{cg} - a) \\ C &= \mu(X_{cg} - a) \\ D &= \mu r_\alpha^2(1 - Z) \end{aligned} \quad (4)$$

or in terms of the primed aerodynamic parameters

$$[D, -C, -B, A] \begin{bmatrix} 1 & 0 & 0 & 0 \\ -a & 1 & 0 & 0 \\ -a & 0 & 1 & 0 \\ a^2 & -a & -a & 1 \end{bmatrix} \begin{bmatrix} L'_1 \\ L'_2 \\ M'_1 \\ M'_2 \end{bmatrix} = BC - AD \quad (5)$$

Equation (5) can be made homomorphic to Eq. (3), i.e.,

$$[D', -C', -B', A'] \begin{bmatrix} L'_1 \\ L'_2 \\ M'_1 \\ M'_2 \end{bmatrix} = B'C' - A'D' \quad (6)$$

by defining the quantities

$$\begin{aligned} A' &= A \\ B' &= B + aA \\ C' &= C + aA \\ D' &= D + aC + aB + a^2A \end{aligned} \quad (7)$$

and requiring that

$$\begin{aligned} A' &= \mu'(1 - R'^2 Z') = \mu(1 - R^2 Z) \\ B' &= \mu'(X'_{cg}) = \mu(X_{cg} - a) + \mu a(1 - R^2 Z) \\ D' &= \mu' r'^2_{\alpha}(1 - Z') = \mu r^2_{\alpha}(1 - Z) + 2a\mu(X_{cg} - a) \\ &\quad + a^2\mu(1 - R^2 Z) \end{aligned} \quad (8)$$

Notice that since $B = C$, $BC - AD = B'C' - A'D'$ and $B' = C'$. The transformations in Eq. (8) allow the definition of a new set of structural parameters μ' , R' , r'_{α} , and X'_{cg} , not unique at this point but homomorphic to the original set. Hence, a solution Z of Eq. (1) can be found by mapping it to the corresponding solution Z' if its dependency on the primed parameters is known.

Simplified Flutter Solutions

The difficulty of solving Eq. (1) for Z comes from the representation of the aerodynamic parameters L_j and M_j . By sampling a number of indicial response curves, Fung¹⁴ observed that a typical indicial lift or moment response $\bar{C}(t)$ to a change of incidence can be adequately represented by $C_{\alpha}(1 - e^{-\lambda t})$, and the corresponding response $H(k)$ to harmonic pitching by $H(k) = C_{\alpha}(1 - ik/\lambda)/[1 + (k/\lambda)^2]$, where k is the reduced frequency based on the chord, t in units of chord traveled, $C_{\alpha} = \bar{C}(\infty)$ or the quasisteady response to α change, $C(t) = \bar{C} - C_{\alpha}$, and

$$\lambda = - \frac{C^2(\infty) - C^2(0)}{2 \int_0^{\infty} C^2 dt}$$

For example, Wagner's function (the Heaviside jump subtracted) can be represented well within 10% by choosing $\lambda = 0.322$ and the corresponding Theodorsen's function within 9 and 35% for the real and imaginary parts, respectively, over the entire range of reduced frequency. It should be noted here that the error measured with respect to a mathematical model, such as Wagner's function, of a physical process does not necessarily imply the same amount of deviation from the physical process.

With Fung's aerodynamic model and the assumption that the downwash $[= \partial h \cdot e^{ikt}/\partial t = kh \cdot e^{i(k t + \pi/2)}]$ due to plunging motion leads that $(= \alpha \cdot e^{ikt})$ of pure (about midchord) pitching motion by $\pi/2$ for low reduced frequencies, the complex aerodynamic coefficients of Eq. (6) take the simple form,

$$L'_1 = L'_{1,r} + iL'_{1,i} = - \frac{2C_{l_{\alpha}}}{\pi[1 + 1/Z\bar{U}\lambda_l^2]\lambda_l} \left[1, \frac{\lambda_l}{k} \right]$$

$$\begin{aligned} L'_2 &= L'_{2,r} + iL'_{2,i} = - \frac{4C_{l_{\alpha}}}{\pi[1 + 1/Z\bar{U}\lambda_l^2]\lambda_l^2} \left[Z\bar{U}\lambda_l^2, -\frac{\lambda_l}{k} \right] \\ M'_1 &= M'_{1,r} + iM'_{1,i} = \frac{4C_{m_{\alpha}}}{\pi[1 + 1/Z\bar{U}\lambda_m^2]\lambda_m} \left[1, \frac{\lambda_m}{k} \right] \\ M'_2 &= M'_{2,r} + iM'_{2,i} = \frac{8C_{m_{\alpha}}}{\pi[1 + 1/Z\bar{U}\lambda_m^2]\lambda_m^2} \left[Z\bar{U}\lambda_m^2, -\frac{\lambda_m}{k} \right] \end{aligned} \quad (9)$$

where $1/k^2$ has been replaced by the complex frequency Z times $\bar{U} [= (U/c\omega_{\alpha})^2]$, the normalized flutter speed square or can be replaced by primed quantities $Z'\bar{U}'$. The comma in the square brackets separates the real and imaginary parts. It is clear from Eq. (9) that the aerodynamic responses of the system are now characterized by two time constants, λ_l and λ_m , and two aerodynamic coefficients, $C_{l_{\alpha}}$ and $C_{m_{\alpha}}$, and that the phase lags between harmonic motions and their aerodynamic responses are simply time delays corresponding to the times for the lift and moment to reach the asymptotic values after a change of α .

Using Eq. (9), the real and imaginary parts of Eq. (1), F_r and F_i , in terms of the primed parameters—it should be noted that the primed and unprimed systems are identical when $a = 0$ —assume the form

$$\begin{aligned} F_r &= R'^2 \mu'^2 r'^2_{\alpha} Z'^2 - (1 + R'^2) \mu'^2 r'^2_{\alpha} Z' + \mu'^2 r'^2_{\alpha} \\ &\quad - \mu'^2 X'_{cg} - L'_{1,r} \mu' r'^2_{\alpha} Z' - M'_{2,r} \mu' R'^2 Z' \\ &\quad + L'_{1,r} \mu' r'^2_{\alpha} + M'_{2,r} \mu' - (L'_{2,r} + M'_{1,r}) \mu' X'_{cg} = 0 \end{aligned} \quad (10)$$

and

$$\begin{aligned} F_i &= -Z' \mu' (L'_{1,i} r'^2_{\alpha} + M'_{2,i} R'^2) + \mu' (L'_{1,i} r'^2_{\alpha} + m'_{2,i}) \\ &\quad - \mu' X'_{cg} (L'_{2,i} + M'_{1,i}) = 0 \\ &= -Z' (L'_{1,i} r'^2_{\alpha} + M'_{2,i} R'^2) + (L'_{1,i} r'^2_{\alpha} + M'_{2,i}) \\ &\quad - [\rho(X_{cg} - a) + a(1 - R'^2 Z')](L'_{2,i} + M'_{1,i}) \end{aligned} \quad (11)$$

where $\rho (= \mu/\mu')$ is chosen and shown later to be independent of μ . Without further substitution of the expressions from Eq. (9) for the L_j and M_j , Eqs. (10) and (11) are exact equivalence of Eq. (1) simplified by a homomorphic transformation. Using the expressions in Eq. (9), they become pure algebraic expressions involving four aerodynamic and five structural parameters for the solution of the flutter speed U and frequency k or, equivalently, \bar{U}' and Z' . Formally, a solution procedure entails iterative selections of \bar{U}' such that Z' satisfies both Eqs. (10) and (11). However, a rather explicit expression for Z' is readily available from Eq. (11), i.e.,

$$Z' = \frac{L'_{1,i} r'^2_{\alpha} + M'_{2,i} - [\rho(X_{cg} - a) + a](L'_{2,i} + M'_{1,i})}{L'_{1,i} r'^2_{\alpha} + M'_{2,i} R'^2 - a R'^2 (L'_{2,i} + M'_{1,i})} \quad (12)$$

which already implies that the circular flutter frequency $\omega (= \omega_{\alpha}/\sqrt{Z'}$ for the case $a = 0$) depends only on the imaginary parts of the aerodynamic parameters and very weakly on μ through the choice of \bar{U}' in Eq. (9) such that Z' satisfies Eq. (10) as well. Again, in this form, despite the simplicity, Eq. (12) is nonetheless exact and is not limited to a particular type of flow. By further assuming that $\lambda_l = \lambda_m$, or $k \ll \lambda_l$ and λ_m , which in general are not equal but of the same order, the denominators in Eq. (9) can be factored out. Thus Eq. (12) reduces to

$$Z' = \frac{A_1 r'^2_{\alpha} + 4A_3 A_4 + [\rho(X_{cg} - a) + a](2A_3 + 2A_1 A_2)}{A_1 r'^2_{\alpha} + 4A_3 A_4 R'^2 + a R'^2 (2A_3 + 2A_1 A_2)} \quad (13)$$

where the aerodynamic parameters C_{l_α} , $1/\lambda_l$, C_{m_α} , and $1/\lambda_m$ have been replaced by A_1 , A_2 , A_3 , and A_4 , respectively, for easy distinction from the primed structural parameters, conveniently defined by setting $\mu' = \mu$, $r_\alpha'^2 = r_\alpha^2 + 2aX_{cg} - a^2$, and

$$R'^2 = \frac{r_\alpha^2 + 2aX_{cg} - a^2}{r_\alpha^2 + a^2R^2} R^2$$

when $r_\alpha^2 + 2aX_{cg} - a^2 \neq 0$. Thus, Z' is related to Z by

$$Z' = \frac{r_\alpha^2 + a^2R^2}{r_\alpha^2 + 2aX_{cg} - a^2} Z$$

and Eq. (10) implies that the flutter reduced frequency k_c , with the subscript c denoting full chord, is given by

$$k_c^2 = \frac{8A_3(1 - R'^2Z') - 4A_1X_{cg}'}{r_\alpha'^2(1 - Z')[\pi\mu'(R'^2Z' - 1) + 2A_1A_2] + \pi\mu'X_{cg}'^2 + 4A_3A_4X_{cg}'} \quad (14)$$

Since the left-hand side is a positive-definite quantity, the right-hand side of this equation explicitly states the condition for flutter. If, however, $r_\alpha^2 + 2aX_{cg} - a^2 = 0$, the choice of

$$\mu' = \frac{r_\alpha^2 + a^2R^2}{r_\alpha^2 - r_\alpha'^2R^2 + a^2R^2} \mu, \quad R'^2 = \frac{r_\alpha'^2}{r_\alpha^2 + a^2R^2} R^2$$

$r_\alpha'^2 = \beta r_\alpha^2$, and a β such that

$$\begin{cases} \beta = 1, r_\alpha^2 - r_\alpha'^2R^2 + a^2R^2 \neq 0 \\ \beta \neq 1, r_\alpha^2 - r_\alpha'^2R^2 + a^2R^2 = 0 \end{cases}$$

yields a different relation for Z and Z' , i.e.

$$Z = \frac{r_\alpha'^2}{r_\alpha^2 - r_\alpha'^2R^2 + a^2R^2} (Z' - 1)$$

and Z' is given by

$$Z' = \frac{2K_1[R'^2a^2X_{cg} + (1 - R'^2)r_\alpha'^2X_{cg} + R'^2r_\alpha'^2a] + (1 + K')(R'^2r_\alpha'^2a^2 + r_\alpha'^4)}{2K_1(R'^4a^3 + R'^2r_\alpha'^2a) + (1 + K'R')(R'^2r_\alpha'^2a^2 + r_\alpha'^4)} \quad (15)$$

where the various A have been replaced by the parameter groups $K' = 4A_3A_4/A_1r_\alpha'^2$ and $K_1 = A_2 + A_3/A_1$. It can be shown that, when $\beta \neq 1$, Z thus computed is independent of the choice of β . Equations (13) and (15) involve five transformed structural parameters and two aerodynamic parameters groups K' and K_1 . Since Z' and then k_c can be computed explicitly, the flutter speed U is simply $c\omega_\alpha/k_c\sqrt{Z}$.

Further simplifications are possible by noting that since the various A are approximately of the same order, the expression for Z' , Eq. (13), depends weakly on a and X_{cg} (assumed small), and setting both to zero reduces Eqs. (13) and (14) to

$$Z = \frac{r_\alpha^2A_1 + 4A_3A_4}{r_\alpha^2A_1 + 4A_3A_4R^2} = \frac{1 + K}{1 + KR^2} \quad (16)$$

$$\begin{aligned} k_c^2 &= \frac{-2(r_\alpha^2A_1 + 4A_3A_4R^2)}{-\pi\mu r_\alpha^2(1 - R^2)A_4 + 2(r_\alpha^2A_1 + 4A_3A_4R^2)A_2A_4} \\ &= \frac{-2(1 + KR^2)A_1/A_4}{-\pi\mu(1 - R^2) + 2(1 + KR^2)A_1A_2} \end{aligned} \quad (17)$$

The condition for flutter, $k_c^2 > 0$, simply requires that the denominator in Eq. (17) be negative and R be less than one—usually the various A are all positive—and, consequently, $k_c \sim 1/\sqrt{\mu}$ for large mass ratio μ . Since Z , also defined as $(k_c U/c\omega_\alpha)^{-2}$, is independent of μ , the flutter speed U must then be proportional to $\sqrt{\mu}$.

Test Cases

We have chosen the computed data and results published in Refs. 16–18 to verify the formulas derived and justify the

assumptions made in the preceding section. First of all, the adequacy of Fung's model is examined by converting the complex aerodynamic coefficients published in these references to their corresponding C_{l_α} , C_{m_α} , λ_l , and λ_m of Eq. (9), which are shown in Figs. 2a–2d with different symbols for different airfoils of different thicknesses or from different references. The agreement between the computed and converted model values is satisfactory for reduced frequencies less than 0.2, as Fung¹⁴ pointed out. It should be noted that the negative value of A_4 in Fig. 2d is due to a violation of the low frequency assumption necessary for Fung's lag model and that there are inconsistencies, especially at high Mach numbers, between the converted values from different references for the same NACA 64A010 airfoil. The effect of these inconsistencies will be discussed later. Figure 3 shows excellent agreement between the flutter boundaries and frequencies obtained using the converted model parameters and a *full* (without the subsequent simplifications) implementation of Eqs. (10) and (11) and those shown in Fig. 8 of Yang et al.¹⁶ for a NACA 64A006 airfoil, $X_{cg} = 0$, $a = -0.5$, $R = 0.1$, $r_\alpha = 0.5$, and three μ .

Since Z is found to depend weakly on μ , the Z values corresponding to $a = 0$ but otherwise the same set of parameters as those in Fig. 3, are plotted on an inverted scale in Fig. 4 together with the Z values for the Cast-7, NACA 64A010, and flat plate airfoil. Unlike the U curves in Fig. 3, the Z curves here show only a weak sensitivity to μ , weaker for larger μ , as evidenced by the smaller difference between the curves for the larger μ than for the smaller μ . Since all cases shown in Fig. 4 are for the same set of structural parameters, the differences in the flutter curves are purely aerodynamic or effects of different airfoil thicknesses. From all data examined and computed for the M_∞ range 0.6–0.9, it is found that k_c has

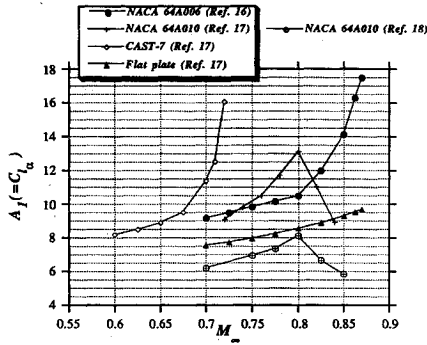


Fig. 2a Lift slopes converted from data in Refs. 16-18.

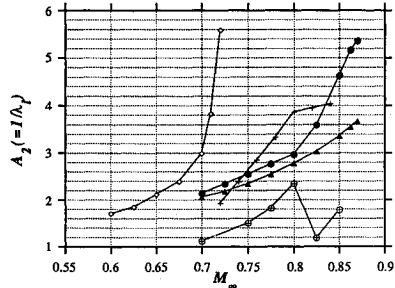


Fig. 2b Lift response times converted from data in Refs. 16-18.

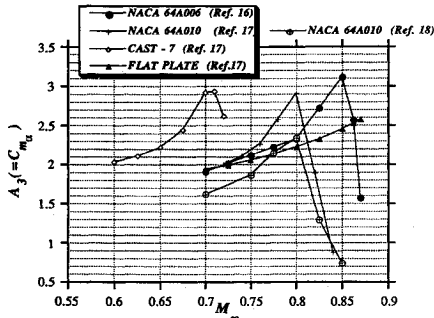


Fig. 2c Moment slopes converted from data in Refs. 16-18.

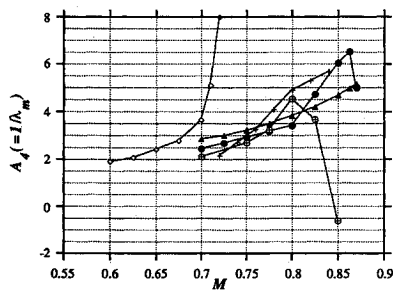


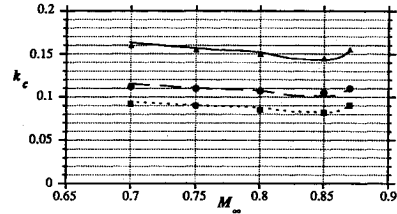
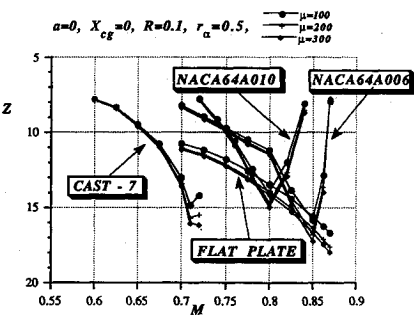
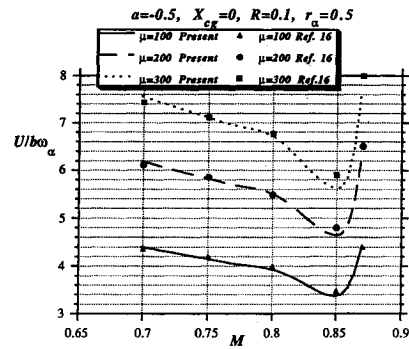
Fig. 2d Moment response times converted from data in Refs. 16-18.

only a weak dependency on M_∞ . Hence, it is advantageous to replace the conventional U vs M_∞ flutter curve with a Z vs M_∞ curve, which is inversely proportional to U^2 but almost independent of μ . It is interesting to note that, for the NACA 64A010 and the same set of structural parameters, $X_{cg} = -0.25$, $a = -0.5$, $R = 0.3$, $r_\alpha = 0.5$, and μ used in Ref. 17, no flutter values were obtained for M_∞ immediately beyond 0.82, precisely as the positiveness of Eq. (17) is violated due to the increased $R = 0.3$ value (from the $R = 0.1$ for the curves in Fig. 4), and no flutter values were shown in Ref. 17 either. Effects of changing other structural parameters on the flutter boundary predicted by Eqs. (10) and (11) are found to be essentially the same as those published by other authors using the classical approach.

As mentioned before, a full implementation of Eqs. (10) and (11) requires iterative guesses of the normalized flutter pressure \bar{U} unless $\lambda_f = \lambda_m$, which in general are of the same order but different, as the values in Figs. 2b and 2d exemplify. Figures 5a and 5b compare results obtained using the *simplified* formulas (13-15) with those using Eqs. (10) and (11) for two choices of a corresponding to the two conditions for Eqs. (13) and (15). The agreement is generally good with only quantitative differences near the dips. It is interesting to note that the frequencies predicted using the simplified formulas are substantially higher near the dip, whereas the full implementation keeps them at about the same as those at lower Mach numbers. It seems that the coupling between Eqs. (10) and (11) makes shallower dips and the flutter frequency rather insensitive to M_∞ . Setting both a and X_{cg} to zero for reasons mentioned earlier and taking advantage of the insensitivity of k_c , the difference between Eqs. (12) and (13), or (15), i.e.,

$$Z_{\text{exact}} - Z_{\text{simp}} = \frac{1 + KF(k_c^2, A_2^2, A_4^2)}{1 + KR^2F(k_c^2, A_2^2, A_4^2)} - \frac{1 + K}{1 + KR^2} \\ = \frac{k_c^2(1 - R^2)K(A_2^2 - A_4^2)}{[1 + KR^2 + k_c^2(A_4^2 + KR^2A_2^2)](1 + KR^2)} \quad (18)$$

where $F(k_c^2, A_2^2, A_4^2) = (1 + k_c^2A_2^2)/(1 + k_c^2A_4^2)$. This shows clearly that the error is proportional to k_c^2 and $K(A_2^2 - A_4^2)$, the latter of which attains its maximum at the dip according to the data in Figs. 2a-2d. Since k_c is usually small for flutter at transonic speeds and is shown earlier to be proportional to $1/\sqrt{\mu}$, the weak and decreasing sensitivity of Z to increasing μ

Fig. 3 Comparison of flutter speeds and frequencies computed using present theory and classical method.¹⁶Fig. 4 Comparison of Z for different μ .

found in Fig. 4 is clear from Eq. (18). Furthermore, this insensitivity to k_c of the flutter speed justifies, as well as explains, the use of a crude model for the aerodynamic response.

Another comparison has been made with the cases Isogai¹⁸ used to study the transonic dip mechanism. Figure 6 compares the flutter speeds and frequencies computed using the full and simplified formulas with those of case B of Isogai¹⁸ for the parameter set of $X_{cg} = 0.2$, $a = -0.3$, $R = 0.2$, $r_\alpha = 0.7$, $\mu = 60$, and A converted from the data shown in Ref. 18. The agreement is generally good. The discrepancies between the full and simplified formulas (the bullets and crosses) are again attributed to the substantial difference between the two aerodynamic time scales A_2 and A_4 , compare the circled crosses in Figs. 2b and 2d. The difference in the predictions of the location of the dip between the present theory and that computed by Isogai (the diamonds) is due to the differences in the various A converted from different harmonic responses of different frequencies. According to Fung's model, there should only be one set of A for all frequencies. However, in practice, the various A converted from different frequencies are different, and the differences are less for those converted from lower frequencies than those from higher ones. It should also be noted that the various A converted from Ref. 17 are more consistent with Fung's model than those converted from Ref. 18 for the same airfoil. The flutter boundary computed using parameters converted from Ref. 17 and the full formulas (the squares in Fig. 6) agrees better with that using parameters converted from Ref. 18 and the simplified formulas (the

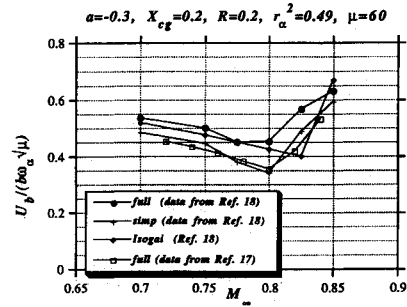


Fig. 6 Comparison of flutter speeds predicted using full and simplified formulas for different data sets.

crosses) than with that using the full formulas (the bullets). The discrepancies simply imply that there are disagreement and inconsistency between the two sets of aerodynamic data computed by different researchers for the same airfoil. Of course, all results shown can be obtained by using A computed directly from indicial responses, instead of converted from known data. However, the conversion from harmonic response of a particular frequency gives a better representation of A for the frequency range, whereas the various A from indicial response are the optimum choice, according to Fung,¹⁴ for all frequencies.

Transonic Dip

Despite its long history and numerous experimental and numerical verifications, a satisfactory explanation has not been available for the most conspicuous phenomenon of flutter, the transonic dip, whose existence is believed to be the result of the large phase lags between structural deformations and their aerodynamic responses. A clear explanation for this phenomenon is explicit in both the simplified and exact expressions for Z , whose strong dependency on the parameter group K implies that the extremum of Z must coincide with that of K . Once this simple fact is known, the location of the dip is simply where K is stationary with respect to M_∞ , i.e.,

$$\begin{aligned} \frac{dZ}{dM_\infty} &= \frac{(1-R^2)}{(1+KR^2)^2} \frac{dK}{dM_\infty} \\ &= \frac{4(1-R^2)K}{(1+KR^2)^2} \left(-\frac{1}{A_1} \frac{dA_1}{dM_\infty} + \frac{1}{A_3} \frac{dA_3}{dM_\infty} + \frac{1}{A_4} \frac{dA_4}{dM_\infty} \right) \end{aligned} \quad (19)$$

or approximately

$$\frac{dZ}{dM_\infty} \approx \frac{4(1-R^2)K}{(1+KR^2)^2 A_3} \frac{dA_3}{dM_\infty} = \frac{4(1-R^2)K}{(1+KR^2)^2 C_{m_\alpha}} \frac{dC_{m_\alpha}}{dM_\infty} \quad (20)$$

since A_3 is substantially smaller than both A_1 and A_4 at transonic speeds. Hence, a simple criterion for the location of the flutter dip is where $(dC_{m_\alpha}/dM_\infty) = 0$, which is predictable using quasisteady results.

All flutter results shown earlier, compare Figs. 2c and 4, as well as others that we have studied, inspected, or computed, agree with this simple criterion. Furthermore, this strong dependency of the flutter dip on the moment slope seems to hold for wings as well. Figure 7 shows computed C_{m_α} values and flutter boundaries using ZUNAS.¹⁹ The dips of both flutter boundaries for the YXX wing computed using either inviscid or viscous (Navier-Stokes) mean flows (as reported in Ref. 20) follow closely the peaks of the corresponding C_{m_α} , despite the substantial shift of dip location due to viscous effects. It appears that the agreement between the inviscid curves is better than that between the viscous curves. This is due to the much smaller dC_{m_α}/dM_∞ when viscous effects are considered than that when viscous effects are ignored. Hence, the terms ignored in Eq. (19) can account for the slight inalignment between the moment slope peak and the flutter dip. If the

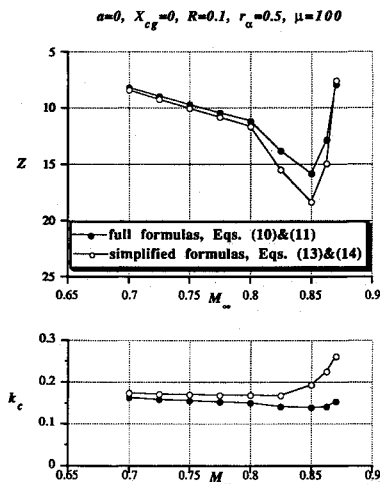


Fig. 5a Comparison of Z and frequencies predicted using full and simplified formulas for $r_\alpha^2 + 2aX_{cg} - a^2 \neq 0$.

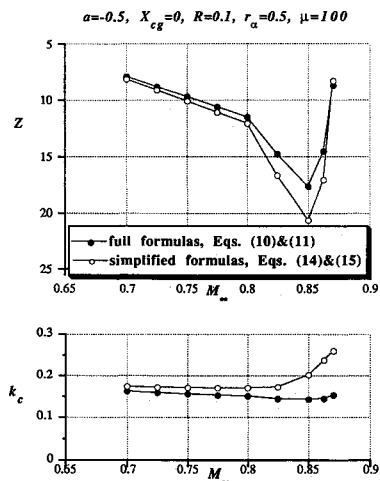
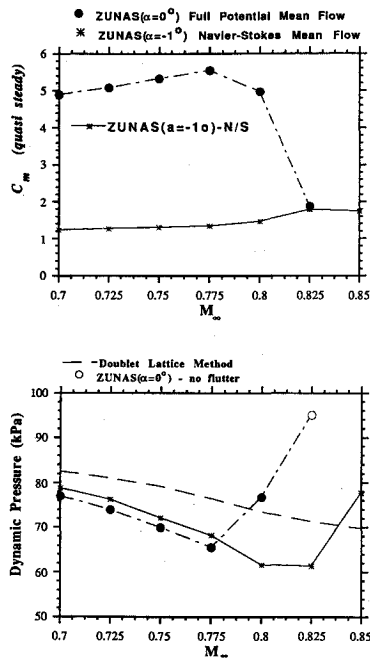
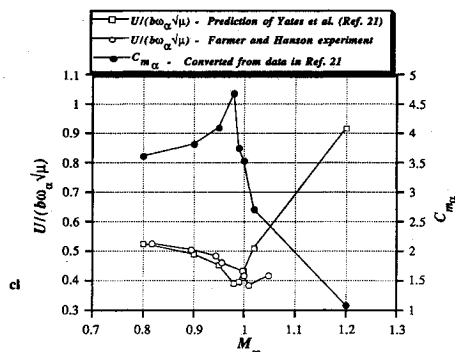


Fig. 5b Comparison of Z and frequencies predicted using full and simplified formulas for $r_\alpha^2 + 2aX_{cg} - a^2 = 0$.

Fig. 7 Computed C_{m_α} peaks and flutter boundary dips.Fig. 8 Measured C_{m_α} peak and flutter boundary dips of Refs. 8 and 21.

variations in the lift slope A_1 were included, the combined moment-slope-over-lift-slope curve would peak at a lower Mach number but closer to the dip than that of the moment slope alone. It should be noted that this C_{m_α} curve was obtained by changing the angle of attack of the entire wing, whereas the flutter points were computed assuming six wing deformation modes, all of which have zero root-chord displacement. The agreement here is, of course, qualitative, but the dominant role of C_{m_α} in flutter prediction is nonetheless clear. Figure 8 shows the same consistency between the dip and the C_{m_α} peak, extracted and integrated from the data published in Refs. 8 and 21, for the TF-8A wing used in the well-known Farmer and Hanson experiment.⁸ However, both Yates' modified strip theory²¹ and the present criterion underpredict the dip location by 0.04 Mach number. Yates et al.²¹ attributed this shift to the difference in model and wind-tunnel sizes between the flutter wing model in the Farmer and Hanson experiment and the pressure wing model in Harris' investigation,²² from which the quasisteady aerodynamic data used for the theoretical predictions originated. Furthermore, it can be inferred from the sensitivity of the moment slope to viscous effects, shown earlier on the YXX wing, that the deformation of the (flexible) flutter wing model⁸ under load can also cause a substantial variation of the moment slope from that measured on the (rigid) pressure wing model.²²

According to the present theory, flutter at transonic speeds depends on two structural parameters, R and r_α , but critically

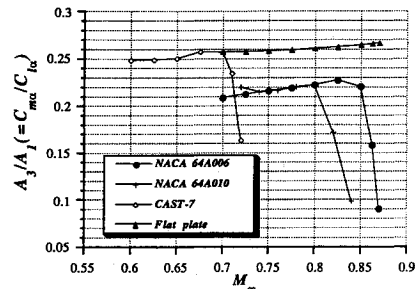


Fig. 9 Variations of moment over lift slopes through transonic Mach numbers.

on the aerodynamic parameter group $C_{m_\alpha}/(\lambda_m C_{L_\alpha})$. At supercritical speeds, these values deviate substantially from those at low Mach numbers or predicted by linearized theory. As exemplified in Fig. 9 for the values in Figs. 2a and 2c, the moment-slope-over-lift-slope ratio is roughly 0.25, corresponding to the quarter-chord location of the aerodynamic center for subsonic Mach numbers as linearized theory predicts, but changes drastically within a narrow range of transonic speeds to small values, corresponding to the movement of the aerodynamic center toward the midchord as the shock moves toward the trailing edge, rendering the flow over the suction side essentially supersonic. Because of the increasing time lag, measured by $1/\lambda_m$, the flutter speed becomes increasingly dependent on the moment slope C_{m_α} , which increases rapidly as the shock appears and decreases sharply as the shock approaches the trailing edge. The transonic dip is simply a manifestation of this purely transonic aerodynamic phenomenon.

Conclusions

It is shown that the two-degree-of-freedom airfoil flutter system is algebraically homomorphic in that solutions about different elastic axes can be made equivalent to that about the midchord by redefinition of the structural parameters. Fung's aerodynamic model for unsteady transonic flow further simplifies the representation of aerodynamic responses and reveals the weak coupling between the flutter dynamic pressure and frequency. Thus, explicit algebraic expressions for the flutter dynamic pressure and frequency with groupings of quasisteady aerodynamic parameters distinct from structural parameters are possible. The expression for the flutter frequency also implies the condition for flutter. Many characteristics of flutter and their parametric dependency are readily discernible from the full as well as the simplified expressions. Extensive comparisons with published results by other authors show excellent agreement between the present approach using a simplified aerodynamic model and the classical approach using numerically integrated nonlinear aerodynamics.

In addition to the usual structural parameters, the present theory characterizes flutter by four aerodynamic parameters, two of which, the lift and moment derivatives, are readily available from quasisteady calculations or measurements and the others, the characteristic time constants of lift and moment responses, from numerical or experimental indicial responses to change of α . Flutter is found to depend critically on the parameter group $C_{m_\alpha}/(\lambda_m C_{L_\alpha})$, and the transonic dip is simply a manifestation of the variation of C_{m_α} with M_∞ .

The theory here suggests that the phenomena of flutter, which are unsteady in nature, can be viewed as a result of the delay in aerodynamic response to a change of position. The conditions at which flutter occurs are determined by the quasisteady stability derivatives modified and enhanced by a measure of this delay.

References

- Regier, A. A., and Martin, D. J., "Recent Experimental Flutter Studies," NACA RM L51F11, June 1951.
- Landahl, M. T., *Unsteady Transonic Flow*, Pergamon, New York,

1961, p. ix.

³Tijdeman, H., "Investigations of the Transonic Flow around Oscillating Airfoil," Doctoral Thesis, Technische Hogeschool Delft, Delft, The Netherlands, Dec. 1977.

⁴Isogai, K., "On the Transonic-Dip Mechanism of Flutter of a Sweptback Wing," *AIAA Journal*, Vol. 17, No. 7, 1979, pp. 793-795.

⁵Isogai, K., "Transonic-Dip Mechanism of Flutter of a Sweptback Wing: Part II," *AIAA Journal*, Vol. 19, No. 9, 1981, pp. 1240-1242.

⁶Ashley, H., "Role of Shocks in the 'Sub-Transonic' Flutter Phenomenon," *Journal of Aircraft*, Vol. 17, No. 3, 1980, pp. 187-197.

⁷Zwann, R. J., "Unsteady Airloads and Aeroelastic Problems in Separated and Transonic Flow," *VKI Lecture Series 1981-4*, von Kármán Inst., Belgium, March 1981.

⁸Farmer, M. G., and Hanson, P. N., "Comparison of Supercritical and Conventional Wing Flutter Characteristics," *Proceedings of the AIAA/ASME/SAE 17th Structures, Structural Dynamics, and Materials Conference*, AIAA, New York, April 1976, pp. 608-611; see also NASA TM X-72837, May 1976.

⁹Albano, E., and Rodden, W. P., "A Doublet-Lattice Method for Calculating Lift Distributions on Oscillating Surfaces in Subsonic Flows," *AIAA Journal*, Vol. 7, No. 2, 1969, pp. 279-285.

¹⁰Chen, P. C., and Liu, D. D., "A Harmonic Gradient Method for Unsteady Supersonic Flow Calculations," *Journal of Aircraft*, Vol. 22, No. 5, 1985, pp. 371-379.

¹¹Theodorsen, T., "General Theory of Aerodynamic Instability and the Mechanism of Flutter," NACA Rept. 496, Jan. 1935.

¹²Kemp, N. H., and Homicz, G., "Approximate Unsteady Thin-Airfoil Theory for Subsonic Flow," *AIAA Journal*, Vol. 14, No. 8, 1976, pp. 1083-1089.

¹³Ballhaus, W. F., and Goorjian, P. M., "Implicit Finite-Difference Computation of Unsteady Transonic Flows About Airfoils,"

AIAA Journal, Vol. 15, No. 12, 1977, pp. 1728-1735.

¹⁴Fung, K.-Y., "A Model for Unsteady Transonic Indicial Responses," *AIAA Journal*, Vol. 20, No. 8, 1982, pp. 1142-1143.

¹⁵Fung, Y. C., *An Introduction to the Theory of Aeroelasticity*, Dover, New York, 1969, pp. 235-244.

¹⁶Yang, T. Y., Guruswamy, P., Striz, A. G., and Olsen, J. J., "Flutter Analysis of a NACA 64A006 Airfoil in Small Disturbance Transonic Flow," *Journal of Aircraft*, Vol. 17, No. 4, 1980, pp. 225-232.

¹⁷Yang, T. Y., Guruswamy, P., and Striz, A. G., "Application of Transonic Codes to Flutter Analysis of Conventional and Supercritical Airfoils," *Proceedings of the AIAA/ASME/ASCE/AHS 22nd Structures, Structural Dynamics, and Materials Conference*, AIAA, New York, April 1981 (AIAA Paper 81-0603).

¹⁸Isogai, K., "Numerical Study of Transonic Flutter of a Two-Dimensional Airfoil," National Aerospace Lab., Rept. TR-617T, Tokyo, July 1980.

¹⁹Shieh, T. H., Schoen, J., and Fung, K.-Y., "Techniques for Accurate, Efficient Computation of Unsteady Transonic Flow," AIAA 29th Aerospace Sciences Meeting, Reno, NV, AIAA Paper 91-0597, Jan. 1991.

²⁰Fung, K.-Y., and Shieh, T. H., "Prediction of Flutter at Transonic Speeds," *4th International Symposium on Computational Fluid Dynamics*, Vol. 4, Univ. of California at Davis, Davis, CA, Sept. 1991, pp. 365-370.

²¹Yates, E. C., Wynne, E. C., Farmer, M. G., and Desmarais, R. N., "Prediction of Flutter for a Supercritical Wing by Modified Strip Analysis and Comparison with Experiment," AIAA Dynamics Specialists, Conf., AIAA Paper 81-0609, April 1981.

²²Harris, C. D., "Wind-Tunnel Investigation of the Aerodynamic Load Distribution of a Supercritical Wing Research Airplane Configuration," NASA TM X-2469, Feb. 1972.